

Synthesis of a Dibromoperylene Phosphoramidite Building Block and Its Incorporation at the 5' End of a G-Quadruplex Forming Oligonucleotide: Spectroscopic Properties and Structural Studies of the Resulting Dibromoperylene Conjugate

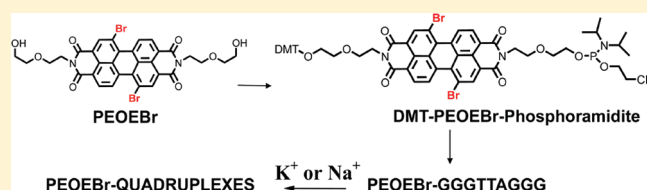
Marco Franceschin,^{‡,§} Nicola Borbone,^{‡,§} Giorgia Oliviero,[†] Valentina Casagrande,[‡] Maria Scutto,[†] Teresa Coppola,[†] Silvia Borioni,[‡] Luciano Mayol,[†] Giancarlo Ortaggi,[‡] Armandodoriano Bianco,[‡] Jussara Amato,[†] and Michela Varra^{*,†}

[†]Dipartimento di Chimica delle Sostanze Naturali, Facoltà di Farmacia, Università degli Studi di Napoli Federico II, via D. Montesano 49, 80131 Napoli, Italy

[‡]Dipartimento di Chimica, Sapienza Università di Roma, Piazzale A. Moro 5, 00185 Roma, Italy

S Supporting Information

ABSTRACT: Previous studies indicate that some perylene bisimide derivatives can drive the assembly of DNA G-quadruplexes, thus suggesting the possible advantage in the adoption of perylene-conjugated G-rich oligonucleotides in biological and biotechnological applications. Nevertheless, the typical poor solubility of perylene bisimides strongly limits the number of suitable chemical strategies to prepare perylene-conjugated oligonucleotides. In order to overcome these difficulties, we employed the earlier described core twisted perylene derivatives possessing unique optical and electronic properties, besides good solubility in common solvents. As a first result, the large-scale synthesis of a new dibromoperylene derivative (PEOEBr) phosphoramidite building block is herein reported. Furthermore, the structural behavior of the conjugated PEOEBr-GGGTTAGGG (HTRp2) human telomeric repeat was investigated by using CD, UV, fluorescence, and gel electrophoresis techniques in desalted water and in K^+ - and Na^+ -containing buffers. We observed that the peculiar property of PEOEBr moieties to form dimers instead of extended aggregates drives the HTRp2 strands toward dimerization and mainly promotes the formation of quadruplex species having both the 5'-ends located at the same side of the structures. However, the counterions present in solutions (K^+ or Na^+) as well as the strand concentration, also contribute to influence the topology and the stoichiometry of formed structures. Furthermore, unlike the unmodified sequence GGGTTAGGG (HTR2), HTRp2 strands quickly associate into G-quadruplexes even in desalted water, as assessed by CD experiments.



INTRODUCTION

G-rich oligonucleotides (GROs) are able to form higher-ordered noncanonical DNA structures, known as G-quadruplexes^{1–3} (herein Qs), on the basis of reverse Hoogsteen-like pairing of four guanines (G-tetrad). Qs currently are among the most studied DNA structures since they are supposed to be involved in important biological functions^{4,5} such as telomere maintenance,^{6,7} DNA–protein recognition,⁸ and protein inhibition.⁹ Furthermore, they represent promising models in biotechnological applications^{10,11} including biosensors^{12,13} and nanomechanical devices.¹⁴ The use of DNA Qs in nanomechanics is encouraged by the stability of Qs in a large variety of experimental conditions. GROs can be chemically modified by covalent linkage to suitable molecules^{15–24} in order to investigate their structural and biological properties. The conjugation has a wide range of advantages, including the thermodynamic stabilization of derived structures^{17,23} and the induction of fluorescence and/or electron transfer properties.²⁴ Typically, conjugated molecules are characterized by the presence of a large aromatic core,

(e.g. porphyrine, pyrene, acridine, and pyrene), capable of interacting with G-tetrads by π – π forces.

Among the great number of molecules potentially suitable for conjugation to GROs, perylene bisimide and its derivatives are of particular interest because their presence could add desired features such as chemical resistance and the propensity to form higher-ordered aggregates, as well as favorable fluorescence and electronic properties.^{25,29,30} Furthermore, a member of this family, PIPER (*N,N'*-bis-[2-(1-piperidino)ethyl]-3,4,9,10-perylenetetracarboxylic bisimide) demonstrated the ability to drive the association of G-rich strands into Qs.²⁷ This mechanism, known as “threading intercalation”, has been extensively studied because of its potential involvement in the inhibition of human telomere elongation by telomerase.^{26–28} Although a variety of DNA structures formed by linked perylene-oligonucleotides

Received: December 2, 2010

Revised: April 11, 2011

Published: June 20, 2011

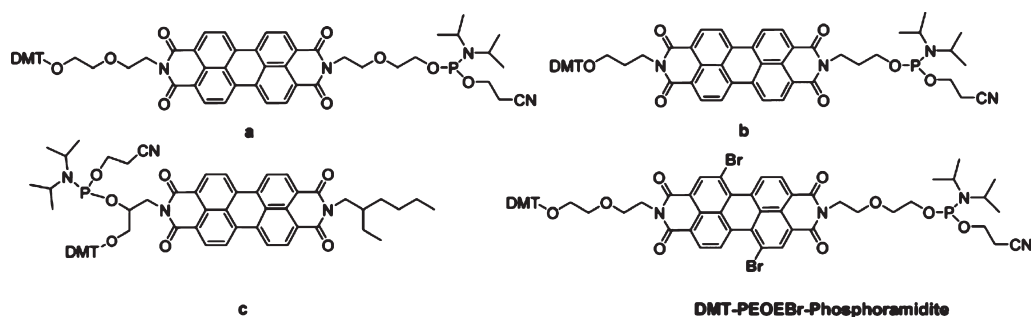


Figure 1. a, b, and c: some previously reported perylene derivative building blocks.^{32,34,37} DMT-PEOEBr-Phosphoramidite: new building block synthesized starting from dibromo-peryene diimide derivative **3d**.

(-ONs), including duplexes,^{31–33} triplexes,³⁴ hairpins, and capped hairpins,^{35–38} have been discussed extensively in many papers, to the best of our knowledge only one perylene bisimide-conjugated GRO has been reported to date.³⁹ For this reason, in this work we explore the properties of DNA Qs formed by perylene-conjugated GROs. To achieve this goal, the synthesis of a perylene bisimide phosphoramidite building block, suitable for subsequent solid-phase functionalization, was required. Despite the poor water solubility of perylene derivatives, some successful conjugations of duplex-forming ONs have been reported in aqueous solutions,^{32,34,37} as the water solubility of perylene moieties significantly improves after association with the target ON. This behavior could probably be ascribed to the presence of the negatively charged phosphate groups on the ON backbone.³¹ However, we did not expect to observe a similar behavior for GROs conjugation, as even unmodified GRO(s) can result in insoluble aggregates,⁴⁰ hence, the importance of developing a new methodology for the synthesis of conjugated perylene-GROs.

The starting point of the synthesis was the formation of a new bromine-substituted perylene bisimide phosphoramidite building block (DMT-PEOEBr-Phosphoramidite, Figure 1), that was incorporated at the 5'-end of the selected GGGTTAGGG (HTR2) human telomeric repeat sequence. The choice of the PEOEBr moiety was due to our previous observation^{41,42} that perylene bisimide derivatives containing suitable groups on the carbocyclic scaffold (known as "bay-area") exhibited greater solubility in aqueous solution. UV, CD, fluorescence, and gel electrophoresis techniques were used in order to investigate the self-assembly properties of the resulting molecule, in which two types of association forces, i.e., strand organization in Qs and perylene derivative aggregation, are potentially involved.

EXPERIMENTAL PROCEDURES

Reagents and Equipment. Chemicals and anhydrous solvents were purchased from Fluka-Sigma-Aldrich. TLCs were run on Merck silica gel 60 F254 plates. Silica gel chromatography was performed by using Merck silica gel 60 (0.063–0.200 mm). API 2000 (Applied Biosystem) and the Micromass Q-TOF MICRO electrospray mass spectrometers were used to acquire the mass data of the intermediates and the monomer. NMR experiments were recorded using Varian NMR spectrometers running at 400 (Mercury Plus) and 500 (UnityINOVA) MHz. Elemental analyses (C, H, N) were carried out on a CE instrument EA1110 CHNS-O (Thermo-Fischer). Reagents and phosphoramidites for DNA synthesis were purchased from Glenn Research. ON syntheses

were performed on a PerSeptive Biosystem Expedite DNA synthesizer. HPLC analyses and purifications were carried out using a JASCO PU-2089 Plus HPLC pump equipped with a JASCO BS-997-01 UV detector. A Purospher-STAR RP-18 end-capped (5- μ m) HPLC column was used to purify the sequences. Both conjugated and unmodified ONs were dialyzed using Slide-A-Lyzer Dialysis Cassettes, with a 3500 molecular weight cutoff, manufactured by Thermo-Scientific. MALDI-TOF experiments were performed on a Bruker Autoflex I mass spectrometer using a picolinic/3-hydroxypicolinic acid mixture as the matrix. The UV thermal experiments were carried out using a JASCO 530 spectrophotometer equipped with ETC-505 T temperature controller. CD experiments were performed on a JASCO 715 spectropolarimeter equipped with a PTC-348 temperature controller. Fluorescence emission spectra were recorded using a Varian Cary Eclipse Fluorescence spectrophotometer (fluorescence data are reported in the Supporting Information). EMSA studies were performed at 4 °C in a Biorad apparatus equipped with Power Pack 3000.

General Procedures for 3a–d. Starting material **2** (500 mg, 0.91 mmol), synthesized as previously described⁴² as a mixture of the two possible isomers, was dissolved in anhydrous *N,N*-dimethylacetamide (10 mL) and 1,4-dioxane (10 mL). The appropriate commercially available amino-alcohol (2 mmol) was added, and the reaction mixture was stirred at 120 °C under argon, for 2 h (2-aminoethanol and 3-amino-1-propanol), 30 min (5-amino-1-pentanol), or 15 min (2-(2-aminoethoxy)ethanol). Upon cooling and water addition, the red solid was washed repeatedly with water, separated by filtration, and dried. To remove the 1,6- from 1,7-dibromo-peryene derivatives, each product **3a–d** was first converted into the corresponding acetyl-derivative, by treatment with acetic anhydride in dry pyridine. The resulting mixtures were dried under vacuum, dissolved in DCM, and washed three times with water. Each organic layer was dried and the residue dissolved in DCM/MeOH (9:1; v/v), from which the 1,7-dibromo-peryene derivatives were selectively precipitated.^{43,44} After three reprecipitations, the desired products were obtained as pure solids, as ascertained by ¹H and ¹³C NMR (Figures 2 and S1–S2 (Supporting Information)). Finally, the acetyl groups were removed by treatment with a mixture of aqueous NH₃ (33%) and MeOH (1:1 v/v, 2 h, r.t.) to give the pure bisimides **3a–d** (Scheme 1).

***N,N'*-Bis(2-hydroxyethyl)-1,7-dibromoperylene-3,4:9,10-tetracarboxylic bisimide (3a).** Reaction yield was 82% (70% after purification of the 1,7 regioisomer). Anal. found C 52.6%, H 2.6%, N 4.3% (calcd for C₂₈H₁₆Br₂N₂O₆: C 52.8%, H 2.5%, N 4.4%). In order to achieve an affordable NMR characterization,

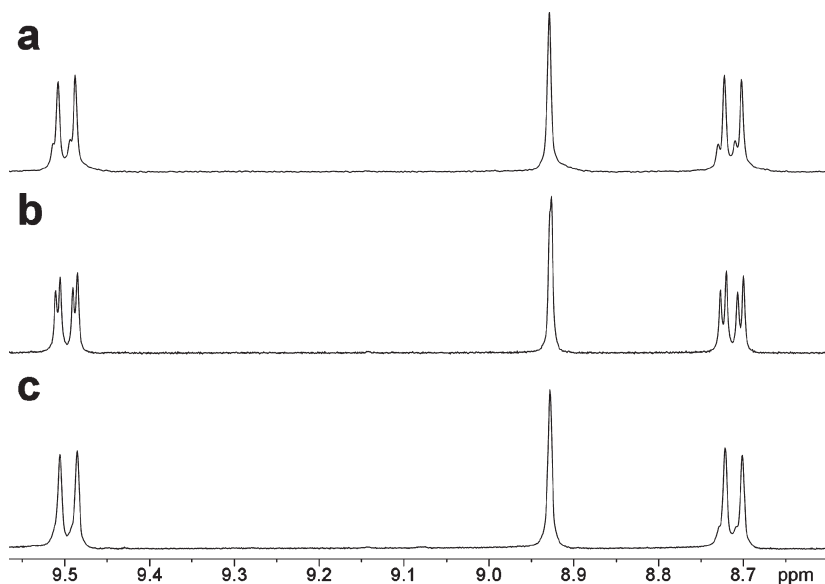
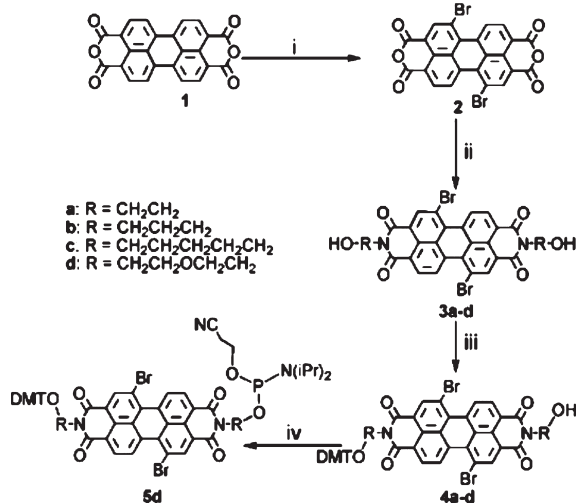


Figure 2. expanded aromatic regions of ^1H NMR spectra in CDCl_3 of (a) a mixture 6:1 of 1,7 and 1,6 regioisomers of acetylated **3d**; (b) mother liquor enriched with the 1,6 regioisomer after precipitation; (c) 1,7 regioisomer of acetylated **3d**. All spectra were registered after two precipitation steps.

Scheme 1. Synthesis of DMT-PEOEBr-Phosphoramidite^a



^a Reagents and conditions: (i) **1** (1 mmol), H_2SO_4 conc. 2 h; I_2 80 °C; Br_2 , 4 h, 100 °C; (ii) **2** (0.91 mmol), HORNH_2 (2 mmol), DMA (10 mL), dioxane (10 mL), under argon, using different reaction times (from 30' up to 2 h) depending on the amine used (see Experimental Procedures section); (iii) **3a–d** (0.5 mmol, 1 equiv), DMT-Cl, (0.280 mmol, 0.6 equiv), DMAP, (0.024 mmol, 0.05 equiv) Py/ACN (3:1 V:V, 5 mL), 1 h 30'; (iv) **4d** (0.241 mmol), $(\text{iPr})_2\text{NP}(\text{OCH}_2\text{CH}_2\text{CN})\text{Cl}$ (0.380 mmol, 90 μL , 1.5 equiv), DIPEA (1 mmol, 180 μL , 4 equiv) in DCM (6 mL), 30'. Only substrate **3d** gave rise to satisfactory yields in DMT-O-derivative **4d**, which, in turn, was converted in the corresponding phosphoramidite building block **5d**.

acetylation of a portion of **3a** was performed (pyridine, 20 h, rt, acetic anhydride) with a yield of 100%. ^1H NMR (400 MHz, CDCl_3): δ 9.46 (d, $J = 8.1$ Hz, 2H, aromatic H), 8.91 (s, 2H, aromatic H), 8.69 (d, $J = 8.1$ Hz, 2H, aromatic H), 4.50 (m, 8H, N- $\text{CH}_2\text{-CH}_2\text{-O}$), 2.03 (s, 6H, acetyl) ppm. MS (ESI) m/z : 740.9466 $[\text{M}+\text{Na}]^+$ (Calcd for $\text{C}_{32}\text{H}_{20}^{79}\text{Br}_2\text{N}_2\text{O}_8\text{-Na}$: 740.9484).

***N,N'*-Bis(3-hydroxypropyl)-1,7-dibromoperylene-3,4:9,10-tetracarboxylic diimide (3b)**. Reaction yield was 89% (75% after purification of 1,7 regioisomer). ^1H NMR (400 MHz, $\text{CDCl}_3/\text{CD}_3\text{OD}$ 9:1): δ 9.42 (d, $J = 8.1$ Hz, 2H, aromatic H), 8.83 (s, 2H, aromatic H), 8.61 (d, $J = 8.1$ Hz, 2H, aromatic H), 4.24 (t, $J = 6.7$ Hz, 4H, $\text{N}_{\text{imidic}}\text{-CH}_2$), 3.60 (t, $J = 6.7$ Hz, 4H, $\text{CH}_2\text{-OH}$), 1.90 (m, 4H, $\text{CH}_2\text{-CH}_2\text{-CH}_2\text{-OH}$) ppm. ^{13}C NMR (100 MHz, 8:2 $\text{CDCl}_3:\text{CD}_3\text{OD}$): δ (referred to CDCl_3) 163.2, 162.8, 138.3, 133.0, 132.8, 130.3, 129.1, 128.5, 127.1, 123.1, 122.0, 121.0, 59.5, 37.7, 30.8 ppm. MS (ESI) m/z : 684.9589 $[\text{M}+\text{Na}]^+$ (calcd for $\text{C}_{30}\text{H}_{20}\text{Br}_2\text{N}_2\text{O}_6\text{Na}$: 684.9586).

***N,N'*-Bis(5-hydroxypentyl)-1,7-dibromoperylene-3,4:9,10-tetracarboxylic diimide (3c)**. Reaction yield was 92% (80% after purification of 1,7 regioisomer). ^1H NMR (400 MHz, CDCl_3): δ 9.47 (d, $J = 8.1$ Hz, 2H, aromatic H), 8.91 (s, 2H, aromatic H), 8.69 (d, $J = 8.1$ Hz, 2H, aromatic H), 4.23 (t, $J = 7.4$ Hz, 4H, $\text{N}_{\text{imidic}}\text{-CH}_2$), 3.69 (t, $J = 6.3$ Hz, 4H, $\text{CH}_2\text{-OH}$), 1.8–1.2 (m, 12H, $\text{CH}_2\text{-CH}_2\text{-CH}_2$) ppm. ^{13}C NMR (100 MHz, CDCl_3): δ 163.2, 162.5, 138.4, 133.2, 131.3, 130.9, 128.8, 128.5, 123.2, 122.4, 121.9, 121.0, 63.0, 40.5, 33.2, 28.0, 23.2. MS (ESI) m/z : 741.0234 $[\text{M}+\text{Na}]^+$ (calcd for $\text{C}_{34}\text{H}_{28}^{79}\text{Br}_2\text{N}_2\text{O}_6\text{Na}$: 741.0212).

***N,N'*-Bis(5-hydroxy-3-oxapentyl)-1,7-dibromoperylene-3,4:9,10-tetracarboxylic diimide (3d)**. Reaction yield was 95% (75% after purification of 1,7 regioisomer). ^1H NMR (400 MHz, CDCl_3): δ 9.38 (d, $J = 8.1$ Hz, 2H, aromatic H), 8.84 (s, 2H, aromatic H), 8.62 (d, $J = 8.1$ Hz, 2H, aromatic H), 4.49 (t, $J = 5.5$ Hz, 4H, N- CH_2), 3.91 (t, $J = 5.5$ Hz, 4H, O- CH_2), 3.72 (m, 8H, O- CH_2) ppm. ^{13}C NMR (100 MHz, CDCl_3): δ 163.2, 162.8, 138.3, 133.0, 132.2, 130.3, 129.2, 128.6, 127.1, 123.1, 122.7, 121.0, 72.6, 68.5, 62.0, 40.2 ppm. MS (ESI) m/z : 744.9830 $[\text{M}+\text{Na}]^+$ (calcd for $\text{C}_{32}\text{H}_{24}^{79}\text{Br}_2\text{N}_2\text{O}_8\text{Na}$: 744.9797). Anal. found C 53.3%, H 3.2%, N 3.8% (calcd for $\text{C}_{32}\text{H}_{24}\text{Br}_2\text{N}_2\text{O}_8$: C 53.1%, H 3.3%, N 3.9%). UV (CHCl_3) λ_{max} nm ($\epsilon \times 10^{-4}$, $\text{M}^{-1}\text{cm}^{-1}$): 492 (3.2), 528 (4.7); UV (DMSO) λ_{max} nm ($\epsilon \times 10^{-4}$, $\text{M}^{-1}\text{cm}^{-1}$): 492 (3.2), 527 (4.6).

General Procedures for 4a–d. Compounds **3a–d** were dried on anhydrous MgCl_2 under vacuum (three days). To each compound (0.5 mmol, 1 equiv), 0.280 mmol of 4,4'-dimethoxytrityl

chloride (0.6 equiv) and 0.024 mmol of 4-dimethylaminopyridine (0.05 equiv) were added. The corresponding 5 mL of the desired mixture of solvents (Py/ACN 3:1 v/v) was added and the solution stirred at room temperature under argon for 1 h. The residual of reactant was then disrupted by the addition of dry methanol. After 10 min, the solvents were removed by vacuum and the crude product dissolved in DCM/TEA (99:1, v/v) and chromatographed on a silica gel column eluted with DCM/MeOH/TEA (99:1:0.5, v/v/v). The resulting yields for each reaction are reported in Table S1 (Supporting Information).

N-2-[(2-*O*-4,4'-Dimethoxytrytilethoxy)ethyl]-*N'*-2-(2-ethoxy)ethyl-1,7-dibromoperylene-3,4,9,10-tetracarboxylic Diimide (**4d**). Yield = 48%. $R_f = 0.4$ (92:8 DCM/MeOH). $^1\text{H NMR}$ (400 MHz, CDCl_3): δ 9.43 (d, $J = 8.0$ Hz, 2H), 8.89 (s, 2H), 8.67 (d, $J = 8.0$ Hz, 2H), 7.27 (5H overlapped by solvent signal), 7.16 (d, $J = 8.8$ Hz, 4H), 6.82 (d, $J = 8.8$ Hz, 4H), 4.48 (t, $J = 5.5$ Hz, 4H), 3.89 (t, $J = 5.5$ Hz, 4H), 3.80 (s, 6H), 3.70 and 3.68 (m, 8H) ppm. $^{13}\text{C NMR}$ (100 MHz, CDCl_3): δ 163.0, 162.6, 158.5, 147.0, 139.4, 138.0, 133.0, 132.8, 130.2, 130.0, 129.1, 128.5, 128.0, 127.7, 127.0, 122.8, 122.4, 120.8, 113.1, 72.2, 68.2, 61.8, 55.2, 45.7, 39.9 ppm. ESI MS m/z : 1063.1 $[\text{M}+\text{K}]^+$ (calcd for $\text{C}_{53}\text{H}_{42}^{79}\text{Br}_2\text{N}_2\text{O}_{10}\text{K}$: 1063.1).

N-2-[(2-*O*-4,4'-Dimethoxytrytilethoxy)ethyl]-*N'*-2-[(2-cyanoethyl)diisopropylphosphino)ethoxy]ethyl-1,7-dibromoperylene-3,4,9,10-tetracarboxylic Diimide (**5d**). Perylene derivative **4d** (0.270 g, 0.241 mmol) was dried *in vacuo* overnight before being dissolved in anhydrous CH_2Cl_2 (6 mL) and 180 μL of diisopropylethylamine (1 mmol, 4 equiv). To this solution, 90 μL (0.380 mmol, 1.5 equiv) of 2-cyanoethyl diisopropylchlorophosphoramidite was added. After 30 min, the reaction mixture was quenched by the addition of dry methanol, diluted with ethyl acetate (10 mL), and washed with 10% sodium carbonate solution (10 mL) and brine (10 mL). The organic layer was dried on magnesium sulfate and concentrated *in vacuo*. The residue was purified on a silica gel column eluted with 80:10:10 v/v/v CH_2Cl_2 /ethyl acetate/TEA. Yield = 95%. $R_f = 0.8$ (80:10:10 in v/v/v CH_2Cl_2 /ethyl acetate/triethylamine). The presence of two PEOBr atropisomers leads the broadening of signals, principally in the aromatic region of $^1\text{H NMR}$ spectra and the splitting of some signals in the $^{13}\text{C NMR}$ spectra. $^1\text{H NMR}$ (400 MHz, CDCl_3) δ 9.47 (br. d, 2H), 8.90 (br. d, 2H), 8.69 (br. d, 2H), 7.31–7.27 (broad, 5H), 7.17 (4H), 6.83 (4H), 4.47 (4H), 4.33–4.23 (m, 2H, $\text{OCH}_2\text{CH}_2\text{CN}$), 3.89 (m, 4H), 3.63 (s, 6H, OCH_3), 3.62–3.58 (8H), 3.40 [m, $J = 6.60$ Hz, 1H, $\text{CH}(\text{CH}_3)_2$], 3.12 (m, 1H, $\text{CH}_2\text{CH}_2\text{CN}$), 2.80 (m, 1H, $\text{CH}_2\text{CH}_2\text{CN}$), 1.28 (d, $J = 6.60$ Hz, 6H, $\text{CH}(\text{CH}_3)_2$). $^{13}\text{C NMR}$ (100 MHz, CDCl_3): δ 162.9, 162.5, 158.5, 145.2, 144.9, 139.4, 138.1, 138.0, 137.7, 135.5, 135.4, 131.0, 130.2, 130.1, 129.6, 129.2, 129.1, 129.0, 128.5, 127.9, 127.8, 127.7, 127.6, 127.0, 126.9, 123.0, 122.5, 120.8, 116.1, 113.1, 112.9, 72.2, 69.5, 68.2, 67.9, 65.4, 63.5, 61.8, 59.6, 55.3, 55.2, 53.0, 45.8, 39.8, 39.5, 29.6, 22.5, 22.3, 20.0, ppm. $^{31}\text{P NMR}$ (200 MHz, CDCl_3 , referenced toward H_3PO_4 85%) δ 147.56, 146.45 (two signals resulting from the splitting of the phosphite signal due to the presence of the dibromoperylene atropisomers^{45,46} (Figure S8, Supporting Information). ESI MS m/z 1225.8 $[\text{M}+\text{H}]^+$ (calcd for $\text{C}_{62}\text{H}_{59}^{79}\text{Br}_2\text{N}_2\text{O}_{11}\text{PH}$: 1225.2).

Synthesis of Oligomers. The ON sequences were synthesized with the above cited automated DNA synthesizer using a controlled pore glass support (100 mg, IcaaCPG high loading, loaded with G nucleotide) following the standard β -cyanoethyl phosphoramidite method (DMT-on protocol). After the elongation of the sequence, the solid support was charged in a small

column supplied with a stopcock and a glass filter on the bottom, washed with dry ACN, fluxed by argon (5 min), and finally treated with three cycles of deblock solution (a solution of dichloroacetic acid in ACN; 5 mL of each cycle) to detach the 4,4'-dimethoxytrityl groups. All of the acidic washing solutions were collected, and the quantitative spectrophotometric 4,4'-dimethoxytrityl cation test⁴⁷ was used to evaluate the yields of each conjugation step. The solid support was washed three times with anhydrous ACN, fluxed by argon (5 min), and then reacted for 20 min with a solution of **5d** in dry DCM, in the presence of the activator solution (5-ethylthio-1H-tetrazole in ACN). After five washing cycles with a 1:1 mixture of dry ACN/DCM, the solid support was dried by argon (5 min) and submitted to the second coupling cycle. The support was washed from the residual excess of reactants by using four swelling cycles in dry solvents under argon flow (2 mL each, for 2 min). The subsequent capping and oxidation cycles were performed manually by using the same conditions of a standard automated synthesis. Finally, the solid support was treated with the deblock solution (five cycles, 5 mL each) to detach the 4,4'-dimethoxytrityl groups. The solid support was then washed with ACN, dried under argon, charged in a vial supplied with a cap, and treated with aqueous ammonia (33%) at room temperature for 24 h to detach the ON. The combined filtrates and washings were concentrated under reduced pressure, dissolved in a basic aqueous solution (2% NH_3), and purified by HPLC by using a C18 reverse phase column [$\text{H}_2\text{O}/\text{ACN}$ 98:2 v/v for 10 min and then by a gradient of ACN in H_2O (from 2 to 20% in 30 min)]. The peaks were identified by setting the UV detector at 260 and 540 nm in two different courses (the conjugated sequence produced a peak at 540 nm). To remove undesired ions, the ON aqueous solutions were subjected to three dialysis treatments (3500 MW cutoff). The concentration of samples used in CD, UV, fluorescence, and electrophoreses experiments were determined by measuring the UV absorbance (at 260 nm, 80 °C) of the aqueous ON solutions, using the extinction coefficient calculated according to the method of Gray et al.⁴⁸ The absorbance contribution of the dibromo-perylene moiety was calculated by using the molar extinction coefficient measured in CHCl_3 (29,500 for the band at 265 nm).

UV and CD Experiments. UV and CD experiments were carried out on DNA samples at concentrations of 2, 4, and/or 10 μM . The buffers used contained 100 mM NaCl and 10 mM NaH_2PO_4 at pH 7.4, or 100 mM KCl and 10 mM KH_2PO_4 at pH 7.4. The samples were annealed by heating at 90 °C for 5 min and then slow cooling at room temperature (12 h). The UV and CD spectra were registered at increasing temperatures, from 10 to 90 °C with heating steps of 10 °C, from 200 to 700 nm. Before each spectrum, the sample was equilibrated for 20 or 30 min, respectively, at the specific temperature. The samples used for the CD measurements of ONs in desalted water (HPLC-grade water, Merck) were not submitted to the annealing procedure. Each reported spectrum is the background-subtracted average of three scans. The spectra were collected with the following conditions: response, 16 s; bandwidth, 1 nm; speed, 100 nm/min.

CD melting curves were obtained by following the changes in the amplitude of CD bands at 263 nm as a function of temperature. ON solutions were heated from 10 to 90 °C, at the rate of 0.5 °C/min.

Electrophoretic Mobility Shift Assay (EMSA). Nondenaturing polyacrilamide gels were performed at 4 °C. The gels

(16%, 29:1 monomer/bis ratio, $10 \times 7.2 \times 0.1$ in size) were run for 3 h at 150 V in 89 mM TBE buffer supplemented with 0.1 M KCl or NaCl. The samples, 0.10 mM of ONs dissolved in 10 mM phosphate buffer containing 100 mM of KCl or NaCl, were annealed by heating at 90 °C for 5 min, slow cooling at 25 °C, and finally storing at 25 °C for 10 days. All unmodified ONs were loaded on gels at the final concentration of 10 μ M, whereas the conjugated HTRp2 sequence was loaded at higher concentrations (50–100 μ M) because of difficulties in staining. The gels were visualized by Biorad Gel DOCXR after SYBR-green staining.

RESULTS

Preparation of Brominated Perylene Bisimide Phosphoramidite Building Block 5d. Dibromo-perylenetetracarboxylic dianhydride (**2**, Scheme 1), synthesized as previously described,^{42,49} was reacted with a series of commercially available amino-alcohols to obtain the bisimides **3a–d**. No side products involving the reaction of hydroxyl groups with the cyclic anhydride were detected. However, the excess of reactants, the temperature, and the reaction times were strictly controlled to avoid bromine substitution with a primary amine (see the Experimental Procedures section).

Each compound **3a–d** was obtained as a mixture of 1,7 and 1,6 dibrominated regioisomers, which, similar to previous reports by Wurthner et al. and Rajasingh et al.,^{46,47} were resolved by selective precipitation. The mixtures of regioisomers **3a–d** were first acetylated and then purified by repetitive precipitation from dichloromethane/methanol (9:1 v/v). The purity of the 1,7 regioisomers was ascertained by ¹H and ¹³C NMR. The ¹H NMR signals of the aromatic portion of the acetylated **3a–d** before and after the purification steps (for an example, see Figures 2 and S1 (Supporting Information)) indicated that the mixtures were efficiently resolved. The acetyl groups were then removed by treatment with a mixture of aqueous NH₃ and MeOH to obtain the 1,7 dibrominated regioisomers **3a–d** (about 90% purity, ascertained by ¹H NMR).

The solubility of derivatives **3a–d** was properly related to the length of the side chains, and it was always higher than that for the corresponding nonbrominated bisimides. The selective introduction of a DMT group was performed by the reaction of **3a–d** with DMT-Cl in the presence of dimethylaminopyridine as a catalyst and a mixture of pyridine-acetonitrile as solvent. Compounds **4a–d** were isolated with yields from 15 to 45%. The reaction yields (Table S1, Supporting Information) were not particularly influenced by the length of the side chains of the perylene bisimides, whereas the presence of an intrachain oxygen significantly affected the reactivity of the hydroxyl group, as suggested by the opposite behavior of **3c** and **3d**. On the basis of these results, **4d** was selected for the conversion in the corresponding phosphoramidite derivative **5d**. The synthesis was carried out by using the classical procedure (95% yields; see the Experimental Procedure section).⁴⁷ The stability of the new phosphoramidite in the standard chemical conditions found in each cycle of the automated solid-phase synthesis was verified prior to its incorporation onto the ON sequence.

Dibromo-Perylene Conjugated ONs. In order to select the best conditions for the coupling step in ON solid phase synthesis, building block **5d** was manually reacted with the commercially available IcaaCPG high-loading solid support functionalized with A, C, G, or T. Upgraded yields were

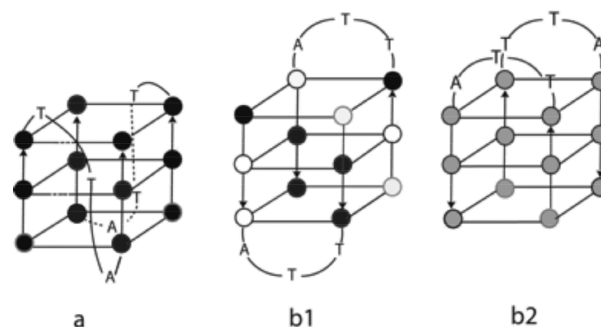


Figure 3. Schematic representation of parallel (a) and antiparallel (b1 and b2) Q structures formed by unmodified HTR2. Black and white balls are used to indicate *anti* and *syn* conformations of dG residues, respectively. The exact orientation of dG residues in the parallel structure has been attributed by X-ray⁵⁵ and NMR results,⁵⁴ whereas in the case of antiparallel b1, by NMR experiments.⁵⁴ The antiparallel form b2 has been determined by biochemical results.⁵³ The N-glycosidic orientation of dG residues has not been determined.

obtained by increasing the time of each coupling cycle from 2 (standard condition) to 20 min (Table S2, Supporting Information). No further improvements were observed by extending the coupling time above 20 min.

The selected sequence HTR2 was first synthesized by automated solid phase synthesis, then manually coupled with **5d** by using two 20 min coupling cycles (Table S2, Supporting Information), and finally detached from the solid support by treatment with 33% aqueous ammonia at room temperature for 48 h (see the Experimental Procedures section). After HPLC purification (Figure S3, Supporting Information), HTRp2 was checked for successful conjugation by MALDI-TOF analyses (Figure S4, Supporting Information).

CD and UV Experiments. The structural behavior of the truncated human telomeric sequence HTR2 has been previously well characterized by using UV, CD, gel electrophoresis, NMR, and X-ray techniques.^{50–55} In K⁺-containing buffer (hereafter in K⁺), HTR2 can form both parallel and antiparallel G-quadruplex structures, which differ by the spatial arrangement of lateral TTA loops (Figure 3). NMR and CD studies^{52–56} evidenced that the two structures can coexist and interconvert in solution. It was also demonstrated that the antiparallel Q arrangement is kinetically favored, while the parallel one corresponds to the thermodynamical one.^{52–56} CD spectra of HTR2 in K⁺ give rise to two positive dichroic bands centered at 263 and 295 nm, which can be ascribed to the formation of a mixture of both parallel and antiparallel Q structures.⁵² Furthermore, in Na⁺-containing solution (hereafter in Na⁺), only antiparallel Q arrangements were observed (b1 and b2, Figure 3).^{52,53} In the latter case, HTR2, possessing a run of guanines at both ends of the sequence, can form at high strand concentration the b2 antiparallel structure (Figure 3), in which the two lateral loops are located on the same side of the Q. Two of these arrangements can mutually interact by π -stacking, forming a dimer of dimers.⁵³ The two-repeat human telomeric sequence carrying additional bases at the ends of the sequence can form only the antiparallel Q in which the two lateral loops TTA are located at opposite sides of the Q structure (b1, Figure 3).⁵⁷ In both cases, CD spectra in Na⁺ give rise to a positive dichroic band centered at 295 nm and a negative one at about 260 nm.

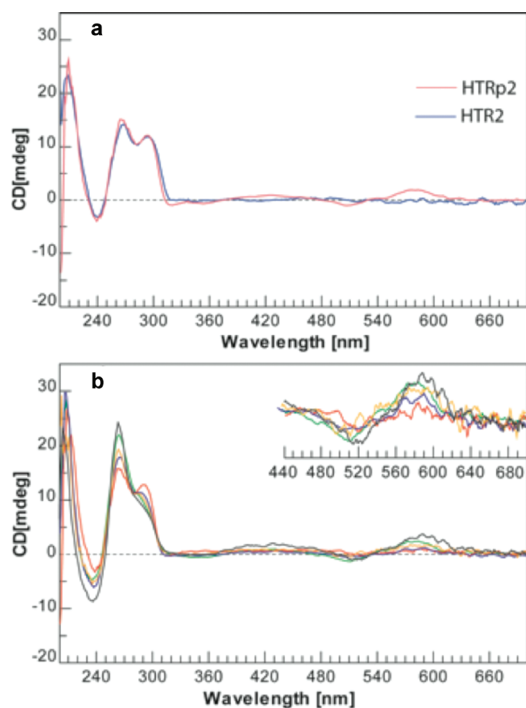


Figure 4. (a) CD profiles of HTRp2 (red, 2 μM) and HTR2 (blue, 2 μM) in 10 mM phosphate buffer (pH 7.4) containing 100 mM of KCl. Both spectra were registered after 12 h from the annealing. (b) Time dependence of CD spectra of HTRp2 (2 μM) in 10 mM phosphate buffer (pH 7.4) containing 100 mM KCl. The sample was heated at 90 $^{\circ}\text{C}$ for 5 min then slowly cooled (12 h) at room temperature, stored at 25 $^{\circ}\text{C}$, and the CD spectra registered at 25 $^{\circ}\text{C}$ after 12 h (red), and 3 (blue), 5 (green), 7 (orange), and 10 (black) days.

In order to verify the effect of perylene conjugation on Q typologies formed by HTR2, CD analyses were performed both in K^+ and in Na^+ . Figure 4 shows the CD profiles obtained from HTRp2 and HTR2 at 10 $^{\circ}\text{C}$ in K^+ . Looking at the similarity of the shape and intensities of dichroic bands observed in the CD spectra of either HTR2 or HTRp2, it appears that the conjugation with the perylene moiety does not significantly affect the topology of resulting Qs. Similarly to HTR2,⁵² the CD profiles of HTRp2 also showed different time-dependent contributions of the two dichroic bands at 262 and 295 nm (Figure 4b), with a constant increase of the first band associated with a constant decrease of the second one. However, according to CD melting experiments (Figure 5a), the conjugation provides a strong stabilizing effect on the parallel Q structure, allowing an increase of the melting temperature of about 30 $^{\circ}\text{C}$.

Furthermore, in K^+ , HTRp2 exhibits strong long-wavelength features in CD profiles (Figure 5b) with a Cotton effect centered at 542 nm (a negative band at 500 nm and a positive band at 565 nm). By increasing the temperature, these CD bands progressively decrease in intensity, completely disappearing at 90 $^{\circ}\text{C}$, whereas the corresponding UV band at 542 nm (Figure 5b) undergoes a strong increase in intensity. The comparison between CD and UV data suggests the existence of exciton coupling between dibromo-perylene moieties.⁵⁶ Interestingly, the CD profile of HTRp2 in Na^+ changed significantly depending on the ON concentration (Figure 6a) and on the time elapsed from annealing (Figure 6b). At low (2 μM) strand concentration, the CD profile showed a positive band at 295 nm and a negative

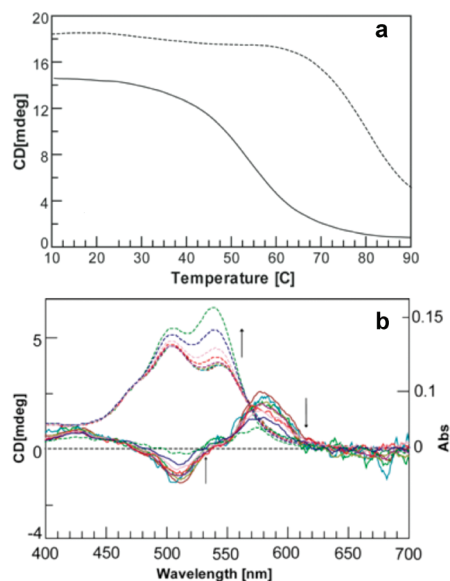


Figure 5. (a) CD melting profiles (at 263 nm) of structures formed by HTR2 (2 μM) (continuous) and HTRp2 (2 μM) (outlined) in 10 mM phosphate buffer (pH 7.4) containing 100 mM of KCl. (b) Temperature-dependent CD and UV profiles in the long wavelength region for HTRp2 in 10 mM phosphate buffer (pH 7.4) containing 100 mM KCl. The arrows indicate the changes in UV and CD bands by increases in the temperature from 10 up to 90 $^{\circ}\text{C}$ with steps of 10 $^{\circ}\text{C}$.

one at 260 nm (Figure 6a, blue line), the same as those for the unmodified HTR2.⁵² By increasing the strand concentration, a new band at 263 nm appeared (Figure 6a, green and red lines). Furthermore, regardless of strand concentration, the band at 295 nm completely disappeared after two days from annealing (Figure 6b). However, in all cases, no significant visible CD bands were observed. The CD melting profile (Figure 6c) obtained by monitoring the intensity of the CD band at 263 nm ($\Delta T = 0.5$ $^{\circ}\text{C}/\text{min}$) showed a strong enhancement in the stability of quadruplex structures formed by HTRp2.

The long-wavelength region of UV profiles (Figure 6d) showed two UV–visible bands produced by the dibromo-perylene moieties. By increasing the temperature from 10 up to 90 $^{\circ}\text{C}$, the band at 542 nm shifted to 538 nm, increasing its intensity. At the same time, its red-broadening disappeared producing an isosbestic point at 570 nm. These observations suggest the existence of exciton coupling between chromophores.^{31–36,56}

Furthermore, the ability of HTRp2 to associate in Q structures in desalted water has also been evaluated. The CD spectra registered after heating at 80 $^{\circ}\text{C}$ and rapidly cooling at 10 $^{\circ}\text{C}$ displayed a positive band at 295 and a negative one at 246 nm (Figure 7a, blue line). At 25 $^{\circ}\text{C}$, the two bands slowly converted, leading after 10 days to the disappearance of the band at 295 nm and to the formation of a new band at 263 nm (Figure 7a, continuous red line). By increasing the temperature, the intensity of the new CD band decreased, and CD profiles showed a mixture of folded and unfolded structures (Figure 7b). These data strongly suggest the formation of Q structures. It is noteworthy that HTR2 did not produce significant CD signals in desalted solution, in agreement with previously reported data (Figure S5, Supporting Information).⁵²

Finally, the short wavelength UV profiles of HTRp2 (Figure S6, Supporting Information), in all explored experimental conditions, showed an isosbestic point at 285 nm according to the

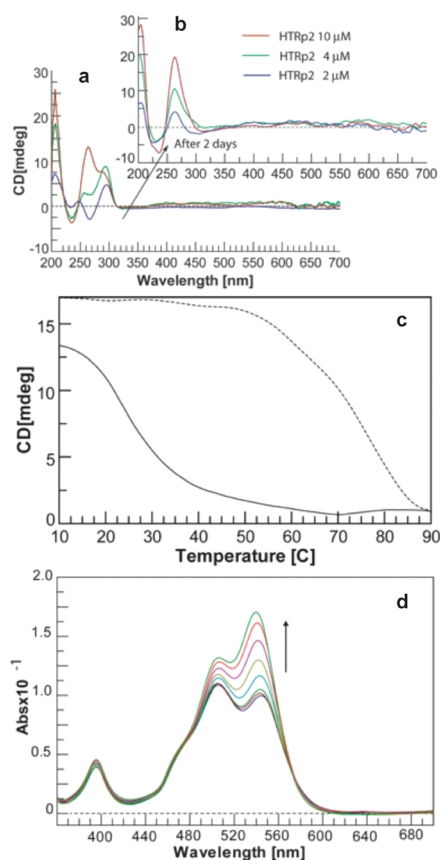


Figure 6. (a) CD spectra of HTRp2 in 10 mM phosphate buffer (pH 7.4) containing 100 mM of NaCl, registered by using different strand concentrations (2, 4, and 10 μM). (b) CD spectra registered by using the same samples after two days. (c) CD melting profiles of structures formed by HTR2 (10 μM) (continuous) and HTRp2 (10 μM) (outlined) in 10 mM phosphate buffer (pH 7.4) containing 100 mM NaCl, registered by positioning the wavelength at 295 and 263 nm, respectively. (d) Long wavelength portion of UV spectra at different temperatures (10–90 $^{\circ}\text{C}$) produced by HTRp2 (4 μM) in 10 mM phosphate buffer (pH 7.4) containing 100 mM of NaCl. The arrow indicates the changes in UV bands by raising the temperature from 10 to 90 $^{\circ}\text{C}$.

presence of Q structures in K^+ , Na^+ , and in water solutions, in agreement with previously reported studies.⁵⁷

EMSA. Figure 8 shows the electrophoresis shift assay for HTRp2 obtained in K^+ . The SYBR-green staining of the bands on these gels required a higher concentration of conjugated ONs than unmodified ones, which have been used as internal standards. This phenomenon could be due to interferences in the stain caused by conjugation with the perylene bisimide moiety. In agreement with CD data, in the presence of K^+ ions, both HTRp2 (lane 4) and HTR2 (lane 3) show a main band. The band corresponding to HTRp2 migrates faster than the tetramolecular Q (TG_4T)₄, used at two different concentrations as the internal standard (lanes 1 and 2), and slightly slower than the bimolecular Q formed from HTR2.⁵² These results are in agreement with the association of HTRp2 in a bimolecular Q, which has a higher molecular weight than that formed from HTR2, according to the presence of two dibromoperylene moieties in the structure. Furthermore, HTRp2 also produced another weak band that migrates near the principal one, suggesting the presence of minor bimolecular Q species. The same study

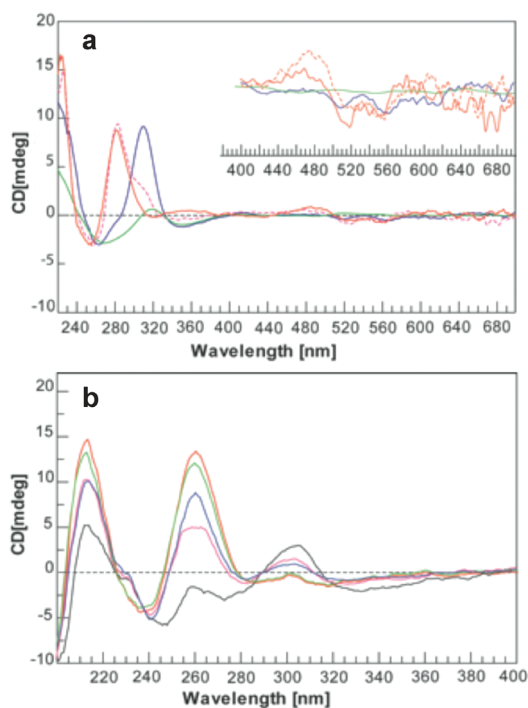


Figure 7. CD and UV spectra of HTRp2 in desalted water. (a) Time dependent CD spectra. The sample was heated at 80 $^{\circ}\text{C}$, rapidly cooled at room temperature (10 min), and kept at 20 $^{\circ}\text{C}$. The spectra were then registered after 1 h (blue line) and 3 days (dashed red line) and 10 days (red line). In green is reported the CD profile of the same sample heated at 80 $^{\circ}\text{C}$. (b) Temperature dependent CD spectra of HTRp2 in water of a sample kept for 10 days at 10 $^{\circ}\text{C}$. The spectra were registered at 10 (red), 20 (green), 40 (blue), 50 (violet), and 80 $^{\circ}\text{C}$ (black).

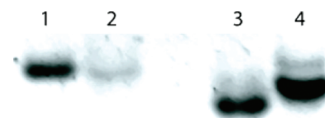


Figure 8. Page experiment on 16% acrylamide gel (acrylamide/bisacrylamide 29:1; running buffer, 89 mM TBE containing 0.1 M KCl). Time course 3 h; 150 V. All samples are annealed in 10 mM phosphate buffer containing 0.1 M KCl. Samples were loaded on gel 10 days after annealing. The gel was stained with Sybr-green for 30 min and visualized by Biorad Gel DOC-XR. Lanes 1 and 2, tetraplex (TG_4T)₄ at 10 and 4 μM , respectively; lane 3, HTR2 ($\text{S}'\text{GGGTTAGGG3}'$) at 10 μM ; lane 4, HTRp2 ($\text{S}'\text{PEOEBR-GGGTTAGGG3}'$) at 50 μM . Prior to loading, all samples were annealed using an ON concentration of 0.1 mM.

did not give significant information in Na^+ , due to the insolubility of the aggregates formed by HTRp2, at the high strand concentration required, that affected the results of PAGE experiments. However, some results (one of these is shown in Figure S7, Supporting Information) account for the formation of higher molecular weight structures, most likely involving four HTRp2 strands.

DISCUSSION AND CONCLUSIONS

Perylene bisimide derivatives show very interesting physical properties that render them useful for a high number of possible technical applications.^{28–30} In order to explore their ability to interact with different DNA structures (duplex, triplex, and

quadruplex), a wide range of perylene conjugated ONs have been synthesized and studied for their physical properties and structural behaviors.^{35–38} Considering the unique structural features of bay-substituted perylene bisimide derivatives,^{41,42,58–60} we have performed the synthesis of a new dibromoperylene phosphoramidite building block, suitable for conjugation with quadruplex-forming GROs, to investigate the effect of such conjugation on the formation of Q species. For this purpose, the Q assembly properties of the 5'-conjugated PEOEBr-HTR2, namely, HTRp2, were evaluated in different conditions using UV, CD, EMSA, and fluorescence methods (discussed in Supporting Information).

The CD data in the short wavelength region showed that in K^+ HTR2 and HTRp2 give rise to similar profiles having two dichroic bands, which can be related to the formation of both parallel and antiparallel Q structures (Figure 4a). We also observed that in K^+ the antiparallel Q formed by HTRp2 slowly switched to the parallel one (Figure 4a), in agreement with previously reported data by Vorlikova and co-workers.⁵² EMSA results (Figure 8) also confirmed the CD data. HTR2 and HTRp2 gave a main band attributable to a parallel dimeric Q structure, which is the predominant conformation present in solution after 10 days of annealing.⁵² Furthermore, the CD-melting behavior in K^+ showed that the unfolding of the Q structures produced by HTRp2 is still incomplete at 90 °C (Figure 5a), thus suggesting a strong stabilizing effect due to PEOEBr conjugation. Conversely, in Na^+ , the shape of CD profiles displayed strong changes by increasing the ON concentration and the time elapsed from annealing (Figure 6). CD spectra registered 3 h after annealing at 2 μM HTRp2 concentration showed profiles closely related to the unmodified HTR2, which could be ascribed to the formation of antiparallel dimeric species. By increasing the strand concentration, the CD profiles progressively changed, and the new profiles could be related to the presence in solution of a mixture of both parallel and antiparallel species. However, 2 days after annealing all of the CD spectra profiles, registered using different strand concentrations, showed only the positive band at 263 nm and the negative one at 243 nm. Furthermore, in desalted water, we observed that HTRp2 produced a time-dependent CD profile (Figure 7) very similar to that obtained in Na^+ , suggesting the higher ability of HTRp2 to assemble into Q structures than the corresponding HTR2. The overall CD results obtained in the short wavelength region suggest that HTRp2 preferentially forms a parallel Q structure in solution, regardless of the presence of salts. Despite the fact that all the UV spectra have similar behaviors in the long wavelength regions, even in different conditions, the CD curves in the same regions were different, depending on the solvent. This aspect will be further investigated. Although it is not possible to explain the nature of these phenomena with only the use of spectroscopic data, it is possible to point out that core twisted perylene derivatives preferentially form dimers instead of extended aggregates.^{25,58–60} Furthermore, the core twisted PEOEBr can generate two enantiomers⁴⁶ that become diastereoisomers when a nitrogen atom of the imide functions is substituted with the ON chain. The low energy of isomerization makes the diastereoisomers produced by the single strand HTRp2 indistinguishable so that the visible CD bands must be attributed to the environment of PEOEBr moieties in the Qs. On this basis, we could hypothesize that the interaction between PEOEBr moieties promotes the dimerization of strands and that the Q typologies formed in solution will be tightly dependent on



Figure 9. Schematic representation of the hypothesized mechanism of strand structuration into parallel Q in K^+ -containing solution. Red circles are used to visualize the G residues carrying the perylene moiety.

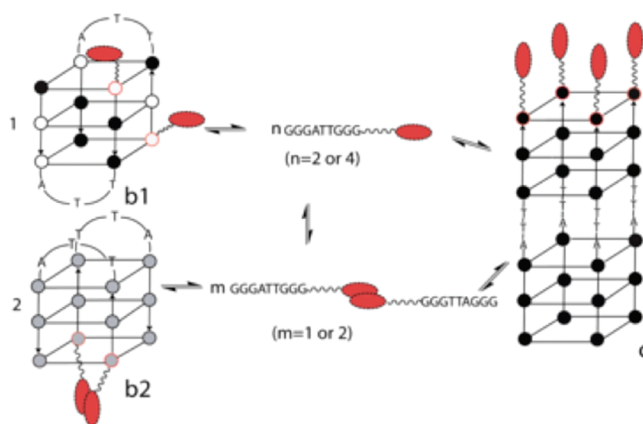


Figure 10. Schematic representation of the hypothesized mechanism of strand structuration into parallel Q in Na^+ -containing solution. At low strand concentration, the kinetic antiparallel Q (b1) is the main structure present in the solution after the annealing; it formed from unstacked dibromoperylene conjugated strands. After reaching equilibrium, the thermodynamic structure c becomes the main Q structure in the solution. At high strand concentration, the Q structures b2 and c are probably formed by the reorganization of dimers of HTRp2. In the latter case, the kinetic antiparallel Q is most likely represented by b2, which in turn, evolves in the thermodynamic Q structure c. Red circles are used to visualize the G residues carrying the perylene moiety.

the association of PEOEBr cores, rather than on the association of two single strands. Consequently, the obtained data could be explained according to the formation of HTRp2 dimers in solution. In fact, in desalted water strand dimerization promotes the folding into Qs, and, due to the poor stability of Qs, there are no forces obstructing the complete conversion of antiparallel into parallel species.

In K^+ , the presence of PEOEBr dimers determines a strong stabilization of Qs, particularly for the parallel bimolecular species, where the two 5'-ends arrange on the same side of the Q structure. The negative–positive signature of the Cotton effect observed in the visible region of CD spectra suggests the presence of a right-handed helical arrangement of PEOEBr units in the structure. It could be hypothesized that the right-handed nature of the helix forces the PEOEBr chromophores to interact with each other following the same helical sense (in Figure 9, a schematic representation of the hypothesized strand association for the HTRp2 parallel Q is reported). Conversely, in Na^+ the existence of HTRp2 dimers obstructs the folding into b1 Q topology (Figure 10), which can only be obtained in solutions containing low ON strand concentration. The HTRp2 association in antiparallel species is a kinetic process. The comparison of time dependent changes occurring in the amplitudes of the

two CD bands at 263 and 295 nm in the explored conditions (Na^+ , K^+ , and desalted water) evidenced that the highest rate of conversion occurs in Na^+ , suggesting that the antiparallel association of HTRp2 in Qs is particularly unfavorable in the latter condition. The thermodynamically stable Q species is formed after about two days from annealing at room temperature, and it could be most likely based on a parallel tetramolecular Q arrangement, as previously reported by Hamilton and co-workers for a perylene-conjugated GRO.³⁹ Differently from K^+ containing solutions, in the presence of Na^+ ions the long wavelength region of CD profiles does not display any dichroic band. These results could be ascribed to compensative effects produced by the different stacking mode of four dibromoperylene moieties at the ends of tetramolecular parallel Q species. Interestingly, unlike the short wavelength region, the long wavelength region of CD spectra seems to be able to discriminate the two Q topologies formed from conjugated ON (Figures 9 and 10).

In conclusion, because of the increased solubility of intermediates in organic solvents, the synthetic transformation of the core twisted PEOEBr derivative into the corresponding phosphoramidite building block is a more efficient and simple process compared to other syntheses involving unsubstituted perylene derivatives. Furthermore, the structural behavior of HTR2 incorporating PEOEBr at its 5'-end seems to be responsible for both the accelerating effect on quadruplex assembly of the resulting molecule in desalted solution and for the strong stabilizing effect of Q structures formed both in Na^+ and in K^+ . In the presence of Na^+ ions, as previously described by Hamilton and co-workers for a perylene-conjugated GRO, the presence of the dibromoperylene moiety promotes the structuration in parallel Qs. However, the decrease in the size of aggregates formed by dibromoperylene moieties, allows also the formation of antiparallel Q species, which have been found to convert into the parallel one in a time- and concentration-dependent manner. All of the phenomena are ascribed to the preference of PEOEBr to form dimers instead of extended aggregates, thus allowing the Q assembly from HTRp2 dimeric species. In our opinion, the introduction of tailored substitutions on the perylene bay area of perylene-conjugated GROs might be a useful tool for the control of the molecularity of resulting Qs since perylene substitution greatly influences the size of perylene aggregates. Moreover, the different CD features shown by PEOEBr moieties could be used as the starting point for the development of new CD methods for the discrimination of different Q structures displaying the same CD profile at short wavelengths. These new CD methods would be particularly suitable also considering that the NMR study of perylene-conjugated GROs in K^+ and in Na^+ is precluded by the formation of insoluble aggregates at the concentration required by the NMR technique (higher than 100 μM). Most likely, this drawback will be overcome by the introduction of tailored substitutions on the perylene bay-area. The synthesis of several PEOEBr-conjugated GROs is currently underway in our laboratories in order to verify the latter hypothesis.

■ ASSOCIATED CONTENT

Supporting Information. Yields of reaction between PEOEBr derivatives 3a–d and DMT-Cl; yields of the coupling step of DMT-PEOEBr-phosphoramidite 5d on functionalized solid supports; ^1H - and ^{13}C NMR spectra of the acetylated 1,7-dibromoperylene derivative 3d; analytical HPLC chromatograms of HTRp2 and HTR2; MALDI-TOF mass spectrum of

HTRp2; PAGE experiment on 16% acrylamide gel; ^{31}P NMR spectrum of DMT-PEOEBr-phosphoramidite 5d; additional UV and CD spectra cited in the text; and fluorescence data (including Figures S9 and S10). This material is available free of charge via the Internet at <http://pubs.acs.org>.

■ AUTHOR INFORMATION

Corresponding Author

*Tel: +39 081 678540. Fax: +39 081 678746. E-mail: varra@unina.it

Author Contributions

⁵These authors contributed equally to this work.

■ ACKNOWLEDGMENT

Funding was provided by Regione Campania (Legge 5), M.I. U.R. (PRIN), and Sapienza Università di Roma. We thank Luisa Cuorvo for technical assistance, Alina Ciammaichella for help in the synthesis of brominated perylene bisimides, Mario Barteri for support in fluorescence measurements, and Caterina Lombardo for precious help in manuscript revision.

■ REFERENCES

- (1) Burge, S., Parkinson, G. N., Hazel, P., Todd, A. K., and Neidle, S. (2006) Quadruplex DNA: sequence, topology and structure. *Nucleic Acids Res.* 34, 5402–5415.
- (2) Simonsson, T. (2001) G-Quadruplex DNA structures variations on a theme. *Biol. Chem.* 382, 621–628.
- (3) Qin, Y., and Hurley, L. H. (2008) Structures, folding patterns, and functions of intramolecular DNA G-Quadruplexes found in eukaryotic promoter regions. *Biochimie* 90, 1149–1171.
- (4) Huppert, J. L. (2008) Hunting G-Quadruplexes. *Biochimie* 90, 1140–1148.
- (5) Maizels, N. (2006) Dynamic roles for G4 DNA in the biology of eucaryotic cells. *Nat. Struct. Mol. Biol.* 13, 1055–1059.
- (6) Paeschke, K., Simonsson, T., Postberg, J., Rhodes, D., and Lipps, H. J. (2005) Telomere end-binding proteins control the formation of G-Quadruplex DNA structures *in vivo*. *Nat. Struct. Mol. Biol.* 12, 847–854.
- (7) Xu, Y., Ishizuka, T., Kurabayashi, K., and Komiyama, M. (2009) Consecutive formation of G-Quadruplexes in human telomeric-overhang DNA: a protective capping structure for telomere ends. *Angew. Chem., Int. Ed.* 48 (42), 7833–7836.
- (8) Bryan, T. M., and Jarstfer, M. B. (2007) Interrogations of G-Quadruplex-protein interactions. *Methods* 43, 332–339.
- (9) Rawal, P., Bhadra, V., Kummarasetti, R., Ravindran, J., Kumar, N., Halder, K., Sharma, R., Mukerji, M., Kumar Das, S., and Chowdhury, S. (2006) Genome wide prediction of G4 DNA as regulatory motifs: role of *Escherichia coli* global regulation. *Genome Res.* 16, 644–655.
- (10) Alberti, P., Bourdoncle, A., Saccà, B., Lacroix, L., and Mergny, J. L. (2006) DNA nanomachines and nanostructures involving quadruplexes. *Org. Biomol. Chem.* 4, 3383–3391.
- (11) Guo, A.-M., and Xiong, S.-J. (2009) Effects of contact and efficient charge transport in G4-DNA molecules. *Phys. Rev.* 80, 035115–1–5.
- (12) Hong, Y., Häubler, M., Lam, J. W. Y., Li, Z., Sin, K. K., Dong, Y., Tong, H., Liu, J., Qin, A., Renneberg, R., and Tang, B. Z. (2008) Label-free fluorescent probing of G-Quadruplex formation and real-time monitoring of DNA folding by a quaternized tetraphenylethene salt with aggregation-induced emission characteristics. *Chem.—Eur. J.* 14, 6428–6437.
- (13) Miranda-Castro, R., de-los-Santos-Alvarez, N., Lobo-Castañón, M. J., Miranda-Ordieres, A. J., and Tuñón-Blanco, P. (2009) Structured nucleic acid probes for electrochemical devices. *Electroanalysis* 21, 2077–2090.

- (14) Deng, M., Zhang, D., Zhou, Y., and Zhou, X. (2008) Highly effective colorimetric and visual detection of nucleic acids using an asymmetrically split peroxidase DNAzyme. *J. Am. Chem. Soc.* **130**, 13095–13102.
- (15) Hayashida, H., Paczesny, J., Juskowiak, B., and Takenaka, S. (2008) Interactions of sodium and potassium ions with oligonucleotides carrying human telomeric sequence and pyrene moieties at both termini. *Bioorg. Med. Chem.* **16**, 9871–9881.
- (16) Jayawickramarajah, J., Tagore, D. M., Tsou, L. K., and Hamilton, A. D. (2007) Allosteric control of self-assembly: modulating the formation of guanine quadruplexes through orthogonal aromatic interactions. *Angew. Chem., Int. Ed.* **46**, 7583–7586.
- (17) Jena, P. V., Shirude, P. S., Okumus, B., Katta, L. -R., Godde, F., Huc, I., Balasubramanian, S., and Ha, T. (2009) G-Quadruplex DNA bound by a synthetic ligand is highly dynamic. *J. Am. Chem. Soc.* **131**, 12522–12523.
- (18) Margulies, D., and Hamilton, A. D. (2009) Digital analysis of protein properties by an ensemble of DNA quadruplexes. *J. Am. Chem. Soc.* **131**, 9142–9143.
- (19) Rosenzweig, B. A., and Hamilton, A. D. (2009) Self-assembly of a four-helix bundle on a DNA quadruplex. *Angew. Chem., Int. Ed.* **48**, 2749–2751.
- (20) Xu, Y., Suzuki, Y., Lonngberg, T., and Komiyama, M. (2009) Human telomeric DNA sequence-specific cleaving by G-Quadruplex formation. *J. Am. Chem. Soc.* **131**, 2871–2874.
- (21) Cai, J., Shapiro, E. M., and Hamilton, A. D. (2009) Self-assembling DNA quadruplex conjugated to MRI contrast agents. *Bioconjugate Chem.* **20**, 205–208.
- (22) Murat, P., Cressend, D., Spinelli, N., Van der Heyden, A., Labbe, P., Dumy, P., and Defranco, E. (2008) A novel conformationally constrained parallel G Quadruplex. *ChemBioChem.* **9**, 2588–2591.
- (23) Cogoi, S., Paramasivam, M., Filichev, V., Geci, L., Pedersen, E. B., and Xodo, L. E. (2009) Identification of a new G-quadruplex motif in the KRAS promoter and design of pyrene-modified G4-decoys with antiproliferative activity in pancreatic cancer cells. *J. Med. Chem.* **52**, 564–568.
- (24) Margulies, D., and Hamilton, A. D. (2009) Protein recognition by an ensemble of fluorescent DNA G-Quadruplexes. *Angew. Chem.* **48**, 1771–1774.
- (25) Würthner, F. (2004) Perylene bisimide dyes as versatile building blocks for functional supramolecular architectures. *Chem. Commun.* **14**, 1564–1579.
- (26) Franceschin, M. (2009) G-Quadruplex DNA structures and organic chemistry: More than one connection. *Eur. J. Org. Chem.* **14**, 2225–2238 and references therein reported.
- (27) Han, H., Cliff, C. L., and Hurley, L. H. (1999) Accelerated assembly of G-quadruplex structures by a small molecule. *Biochemistry* **38**, 6981–6986.
- (28) Tuesuwan, B., Kern, J. T., Thomas, P. W., Rodriguez, M., Li, J., David, W. M., and Kerwin, S. M. (2008) Simian virus 40 large T-antigen G-quadruplex DNA helicase inhibition by G-quadruplex DNA-interactive agents. *Biochemistry* **47**, 1896–1909.
- (29) Imahori, H., Umeyama, T., and Ito, S. (2009) Large π -aromatic molecules as potential sensitizers for highly efficient dye-sensitized solar cells. *Acc. Chem. Res.* **42**, 1809–1818.
- (30) Chen, Z., Lohr, A., Saha-Möller, C. R., and Würthner, F. (2009) Self-assembled pi-stacks of functional dyes in solution: structural and thermodynamic features. *Chem. Soc. Rev.* **38**, 564–584.
- (31) Baumastark, D., and Wagenknecht, H. A. (2008) Perylene bisimide dimers as fluorescent “glue” for DNA and for base-mismatch detection. *Angew. Chem., Int. Ed.* **47**, 2612–2614.
- (32) Wagner, C., and Wagenknecht, H. -A. (2006) Perylene-3,4:9,10-tetracarboxylic acid bisimide dye as an artificial DNA base surrogate. *Org. Lett.* **8**, 4191–4194.
- (33) Baumastark, D., and Wagenknecht, H. A. (2008) Fluorescent hydrophobic zippers inside duplex DNA: Interstrand stacking of perylene-3,4:9,10-tetracarboxylic acid bisimides as artificial DNA base dyes. *Chem.—Eur. J.* **14**, 6640–6645.
- (34) Bevers, S., Schutte, S., and McLaughlin, L. W. (2000) Naphthalene- and perylene-based linkers for the stabilization of hairpin triplexes. *J. Am. Chem. Soc.* **122**, 5905–5915.
- (35) Lewis, F. D., Zhang, L., Kelley, R. F., McCamant, D., and Wasielewski, M. R. (2007) A perylenedicarboxamide linker for DNA hairpins. *Tetrahedron* **63**, 3457–3464.
- (36) Zheng, Y., Long, H., Schatz, G. C., and Lewis, F. D. (2006) A cooperative beads-on-a-string approach to exceptionally stable DNA triplexes. *Chem. Commun.* **29**, 3830–3832.
- (37) Rahe, N., Rinn, C., and Carell, T. (2003) Development of donor–acceptor modified DNA hairpins for the investigation of charge hopping kinetics in DNA. *Chem. Commun.* **17**, 2120–2121.
- (38) Hariharan, M., Zheng, Y., Long, H., Zeidan, T. A., Vura-Weiss, J., Wasielewski, M. R., Schatz, G. C., and Lewis, F. D. (2009) Hydrophobic dimerization and thermal dissociation of perylenediimide-linked DNA hairpins. *J. Am. Chem. Soc.* **131**, 5920–5929 and references reported therein.
- (39) Saha, S., Cai, J., Eiler, D., and Hamilton, A. D. (2010) Programming the formation of DNA and PNA quadruplexes by π – π stacking interactions. *Chem. Commun.* **46**, 1685–1687.
- (40) Mergny, J. L., De Cian, A., Ghelab, A., Saccà, B., and Lacroix, L. (2005) Kinetics of tetramolecular quadruplexes. *Nucleic Acids Res.* **33**, 81–94 and references reported therein.
- (41) Alvino, A., Franceschin, M., Cefaro, C., Borioni, S., Ortaggi, G., and Bianco, A. (2007) Synthesis and spectroscopic properties of highly water-soluble perylene derivatives. *Tetrahedron* **63**, 7858–7865.
- (42) Franceschin, M., Alvino, A., Ortaggi, G., and Bianco, A. (2004) New hydrosoluble perylene and coronene derivatives. *Tetrahedron Lett.* **45**, 9015–9020.
- (43) Würthner, F., Stepanenko, V., Chen, Z., Saha-Möller, C. R., Kocher, N., and Stalke, D. (2004) Preparation and characterization of regioisomerically pure 1,7-disubstituted perylene bisimide dyes. *J. Org. Chem.* **69**, 7933–7939.
- (44) Rajasingh, P., Cohen, R., Shirman, E., Shimon, L. J. W., and Rybtchinski, B. (2007) Selective bromination of perylene diimides under mild conditions. *J. Org. Chem.* **72**, 5973–5979.
- (45) Gryaznov, S. M., and Letsinger, R. L. (1992) Selective O-phosphorylation with nucleoside phosphoramidite reagents. *Nucleic Acids Res.* **20**, 1879–1882.
- (46) Osswald, P., and Würthner, F. (2007) Effects of bay substituents on the racemization barriers of perylene bisimides: Resolution of atropo-enantiomers. *J. Am. Chem. Soc.* **129**, 14319–14326.
- (47) Sinha, N. D., Biernat, J., McManus, J., and Koster, H. (1984) Polymer support oligonucleotide synthesis XVIII: Use of *ss*-cyanoethyl-N,N-dialkylamino-/N-morpholino phosphoramidite of deoxynucleosides for the synthesis of DNA fragments simplifying deprotection and isolation of the final product. *Nucleic Acids Res.* **12**, 4539–4557.
- (48) Gray, D. M., Hung, S. H., and Johnson, K. M. (1995) Absorption and circular dichroism spectroscopy of nucleic acid duplexes and triplexes. *Methods Enzymol.* **246**, 19–34.
- (49) Rohr, U., Schlichting, P., Böhm, A., Gross, M., Meerholz, K., Bräuchle, C., and Müllen, K. (1998) Liquid crystalline coronene derivatives with extraordinary fluorescence properties. *Angew. Chem., Int. Ed.* **37**, 1434–1437.
- (50) Mergny, J. L., Phan, A. T., and Lacroix, L. (1998) Following G-quartet formation by UV-spectroscopy. *FEBS Lett.* **435**, 74–78.
- (51) Mergny, J. L., and Lacroix, L. (2003) Analysis of thermal melting curves. *Oligonucleotides* **13**, 515–537.
- (52) Vorlíčková, M., Chládková, J., Kejnovská, I., Fialová, M., and Kypr, J. (2005) Guanine tetraplex topology of human telomere DNA is governed by the number of (TTAGGG) repeats. *Nucleic Acids Res.* **33**, 5851–5860.
- (53) Balagurumoorthy, P., and Brahmachari, S. K. (1994) Structure and stability of human telomeric sequence. *J. Biol. Chem.* **34**, 21858–21869.
- (54) Phan, A. T., and Patel, D. J. (2003) Two-repeat human telomeric d(TAGGGTTAGGGT) sequence forms interconverting

parallel and antiparallel G-quadruplexes in solution: Distinct topologies, thermodynamic properties, and folding/unfolding kinetics. *J. Am. Chem. Soc.* 125, 15021–15027.

(55) Parkinson, G. N., Lee, M. P. H., and Neidle, S. (2002) Crystal Structure of Parallel Quadruplexes from Human Telomeric DNA. *Nature* 417, 876–880.

(56) Zheng, Y., Long, H., Schatz, G. C., and Lewis, F. D. (2005) Duplex and hairpin dimer structures for perylene diimide–oligonucleotide conjugates. *Chem. Commun.* 38, 4795–4797.

(57) Mergny, J. L., Li, J., Lacroix, L., Amrane, S., and Chaires, J. B. (2005) Thermal difference spectra: a specific signature for nucleic acid structures. *Nucleic Acids Res.* 33, e138/1–6.

(58) Würthner, F. (2006) Bay-substituted perylene bisimides: Twisted fluorophores for supramolecular chemistry. *Pure Appl. Chem.* 78, 2341–2349.

(59) Kaiser, T. E., Stepanenko, V., and Würthner, F. (2009) Fluorescent J-aggregates of core-substituted perylene bisimides: studies on structure-property relationship, nucleation-elongation mechanism, and sergeants-and-soldiers principle. *J. Am. Chem. Soc.* 131, 6719–6732.

(60) Zhang, X., Rehm, S., Safont-Sempere, M. M., and Würthner, F. (2009) Vesicular perylene dye nanocapsules as supramolecular fluorescent pH sensor systems. *Nat. Chem.* 1, 623–629.